Combined SANS and SAXS studies on alkali metal dodecyl sulphate micelles

2007 J. Phys.: Condens. Matter 19 196219

(http://iopscience.iop.org/0953-8984/19/19/196219)

IOP PUBLISHING JOURNAL OF PHYSICS: CONDENSED MATTER

J. Phys.: Condens. Matter **19** (2007) 196219 (9pp) doi:10.1088/0953-8984/19/19/196219

Combined SANS and SAXS studies on alkali metal dodecyl sulphate micelles

J V Joshi[1], **V K Aswal**[2] **and P S Goyal**[1]

[1] UGC-DAE-CSR, Mumbai Centre, Bhabha Atomic Research Centre, Mumbai 400085, India
[2] Solid State Physics Division, Bhabha Atomic Research Centre, Mumbai 400085, India

E-mail: jvjoshi@barc.gov.in

Received 12 February 2007, in final form 21 March 2007
Published 20 April 2007
Online at stacks.iop.org/JPhysCM/19/196219

Abstract

Combined small-angle neutron scattering (SANS) and small-angle x-ray scattering (SAXS) studies have been performed on charged micelles of anionic surfactants of alkali metal dodecyl sulphate (MDS, M = Li, Na, Rb and Cs) in aqueous solution. The dimensions of the micelles have been obtained using SANS as the neutrons are mostly scattered by the hydrogenous core of the micelles. The contrast for the head groups and the counterions is very small, so they are not seen with the neutrons. On the other hand, x-rays are scattered by the electron density fluctuation, which is proportional to the atomic number, and thus x-rays have been used to see the high-Z components of the micelles directly. SAXS from LiDS gives the headgroup thickness, and the counterion condensation is measured directly by the scattering from the high-Z counterions of MDS (M = Na, Rb and Cs) micelles. Based on the results of these two techniques, the role of the different counterions in deciding the structure of micelles has been explained in terms of counterion condensation and the thickness over which they are condensed around the charged micelle. It is found that as the hydrated size of the counterion decreases, the counterion condensation increases and counterions are condensed over a smaller thickness, which results in larger charge neutralization and hence a larger size of the micelles.

1. Introduction

Surfactant molecules in aqueous solution self-associate to form micelles [1–7]. Surfactant molecules such as sodium dodecyl sulphate (NaDS) ionize in aqueous solution and the corresponding micelles are aggregates of dodecyl sulphate (DS^-) ions. The micelle is negatively charged and the Na^+ ions, known as counterions, tend to stay near the DS^- micellar surface. The counterions situated at the vicinity of the colloidal surface experience a very strong electrostatic attraction compared with the thermal energy k_BT, and these counterions

are referred to as being condensed on the colloid surface [8–10]. In charged micellar solutions, counterion condensation plays a very important role in deciding the effective charge on the micelle and hence the formation, structure and interaction of the micelles [1–7].

Micelles of the anionic surfactant of metal dodecyl sulphate (MDS, M = Li, Na, Rb and Cs) show different sizes, although their hydrocarbon chains and head groups are the same [11–14]. This difference in size of the micelles is attributed to the difference in condensation of the counterions around the micelles. The counterions neutralize the charge on the surface of the micelle, which is formed of oppositely charged entities. The distribution of the counterions around the micelles is strongly dependent on the hydrated ionic size of the counterions of the corresponding alkali metal. The hierarchy of the hydrated sizes of the counterions of the alkali metals is given by the Hoffmeister series ($Li^+ > Na^+ > K^+ > Rb^+ > Cs^+$) [7]. In this paper, we show a combined use of SANS and SAXS for the direct observation of counterion condensation on charged micellar solutions of anionic surfactants with different counterions, MDS, and their correlation in deciding the size of the micelles.

Small-angle scattering covers a length scale where most of the micelle structures, starting from spherical to rod-like or disk-like shapes, are formed [15–18]. Small-angle neutron scattering (SANS) and small-angle x-ray scattering (SAXS) in combination provide a direct method for studying the counterion condensation on charged micelles [19–22]. While neutron scattering in micellar solutions is from the core of the micelle, x-rays are largely scattered by counterions, especially when the counterion has a large atomic number Z (e.g. Br^-, Cs^+). The neutron scattering intensity from the counterion distribution is negligible in comparison with that from the core. Thus neutrons see the core of the micelle, and x-rays give information relating to the counterion condensation around the micelle.

2. Experimental details

Lithium dodecyl sulphate (LiDS), rubidium dodecyl sulphate (RbDS) and caesium dodecyl sulphate (CsDS) were synthesized by standard repeated crystallization of solutions of sodium dodecyl sulphate (NaDS) with the corresponding salts. All the chemicals used (NaDS, LiCl, RbCl and CsCl) were obtained from Aldrich. The samples were prepared by dissolving known amounts of surfactants in D_2O. For SANS experiments, deuterium oxide (D_2O) is used as a solvent instead of H_2O, which provides better scattering contrast in neutron scattering experiments. D_2O (99.4% atom) was obtained from Heavy Water Board, BARC, Mumbai, India. In SAXS experiments, the choice of solvent (D_2O or H_2O) does not matter from the point of view of the contrast. However, since the micellar size is significantly different for D_2O and H_2O as solvents [23], D_2O was used for SAXS experiments too. Small-angle neutron scattering experiments were performed using the SANS diffractometer at BARC [24]. The wavelength (λ) of the neutron beam was 5.2 Å. SAXS experiments were performed at the high-brilliance SAXS beamline of the synchrotron source of the European Synchrotron Radiation Facility (ESRF), Grenoble, France [25]. The wavelength (λ) of the x-ray beam was 1.54 Å. For both SANS and SAXS, data were recorded in the Q range of 0.018–0.3 $Å^{-1}$. Measurements were made on micellar solutions of fixed surfactant concentration at 0.3 M. The sample temperature was maintained at 30 °C for all the measurements. The data were corrected using a standard procedure for background, empty-cell contribution and sample transmission.

3. Small-angle scattering analysis

Excluding differences which arise due to characteristics of the radiation used, i.e. neutrons for SANS and x-rays for SAXS, the experimental details and the data analysis methods used for both small-angle scattering techniques (SANS and SAXS) are similar [26]. The difference

between the interactions of neutrons and x-rays with matter gives rise to the different contrasts for the radiation. In a small-angle scattering experiment the measured scattering intensity as a function of wavevector transfer Q ($=4\pi \sin\theta/\lambda$, where 2θ is the scattering angle and λ is the wavelength of the incident radiation) for the micellar solution can be expressed as [27, 28]

$$\frac{\mathrm{d}\Sigma}{\mathrm{d}\Omega}(Q) = n\left[\langle F(Q)^2\rangle + \langle F(Q)\rangle^2 (S(Q)-1)\right] + B \tag{1}$$

where n is the number density of particles. $F(Q)$ is the single-particle form factor, which depends on the shape and size of the particles. $S(Q)$ is the inter-particle structure factor and is decided by the spatial distribution (interaction) of the scattering particles. B is a constant term that represents the incoherent scattering background, which occurs in the case of neutrons mainly due to hydrogen in the sample.

The prolate ellipsoidal shape ($a \neq b = c$) of the micelles is widely used in the analysis of small-angle scattering data, because it also represents the other different possible shapes of the micelles such as spherical ($a = b$) and rod-like ($a \gg b$). For such an ellipsoidal micelle [29]

$$\langle F^2(Q)\rangle = \int_0^1 \left[F(Q,\mu)^2\,\mathrm{d}\mu\right] \tag{2}$$

$$\langle F(Q)\rangle^2 = \left[\int_0^1 F(Q,\mu)\,\mathrm{d}\mu\right]^2 \tag{3}$$

$$F(Q,\mu) = (\rho_\mathrm{m} - \rho_\mathrm{shell})V_\mathrm{m}\left[\frac{3j_1(x_\mathrm{m})}{x_\mathrm{m}}\right] + (\rho_\mathrm{shell} - \rho_\mathrm{s})V_\mathrm{t}\left[\frac{3j_1(x_\mathrm{t})}{x_\mathrm{t}}\right] \tag{4}$$

$$j_1(x) = \frac{(\sin x - x\cos x)}{x^2} \tag{5}$$

$$x_\mathrm{m} = Q[a^2\mu^2 + b^2(1-\mu^2)]^{1/2} \tag{6}$$

$$x_\mathrm{t} = Q[(a+t)^2\mu^2 + (b+t)^2(1-\mu^2)]^{1/2} \tag{7}$$

where ρ_m, ρ_shell and ρ_s are the scattering length densities of the micelle, counterions shell and solvent, respectively. The dimensions a and b are the semi-major and semi-minor axes of the ellipsoidal micelle, respectively, and t is the thickness of the shell of condensed counterions on the micelle. V_m ($=4\pi ab^2/3$) and V_t ($=4\pi(a+t)(b+t)^2/3$) are the volumes of the micelle and total volume of micelle along with shell, respectively. The variable μ is the cosine of the angle between the directions of a and the wavevector transfer Q.

The expression for $S(Q)$ depends on the relative positions of the particles. In the case of the isotropic system, $S(Q)$ can be written as [30]

$$S(Q) = 1 + 4\pi n \int (g(r)-1)\frac{\sin Qr}{Qr} r^2\,\mathrm{d}r \tag{8}$$

where $g(r)$ is the radial distribution function and it gives the probability of finding another particle at a distance r from a reference particle centred at the origin. The details of $g(r)$ depend on the interaction potential $U(r)$ between the particles. For the results reported herein, $U(r)$ was assumed to be the screened Coulomb potential and $S(Q)$ was calculated under the mean spherical approximation [31]. The charge on the micelles is an independent additional interaction parameter, as determined in the calculation of $S(Q)$.

The dimensions of the micelle, aggregation number and the fractional charge have been determined from the analysis of SANS data. The semi-major axis (a), semi-minor axis ($b = c$) and the fractional charge ($\alpha = Z/N$, where Z is the micellar charge and N is the aggregation number) are the parameters in analysing the SANS data. The aggregation number is calculated by the relation $N = 4\pi ab^2/3v$, where v is the volume of the monomer of the surfactant. The above structure and interaction information about the micelles, as obtained from SANS, is used

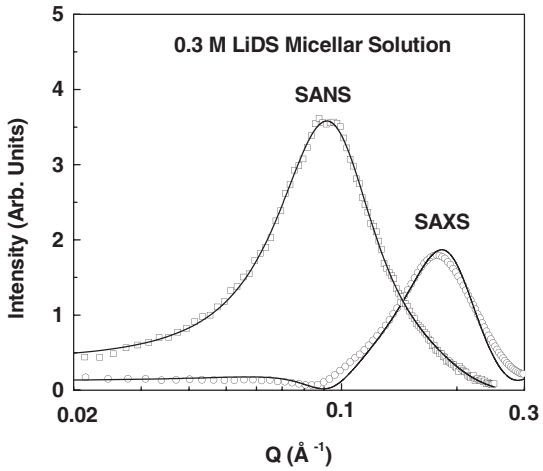

Figure 1. SANS and SAXS data from 0.3 M LiDS micellar solution. Points represent the experimental data and the solid lines are the theoretical fits to the data.

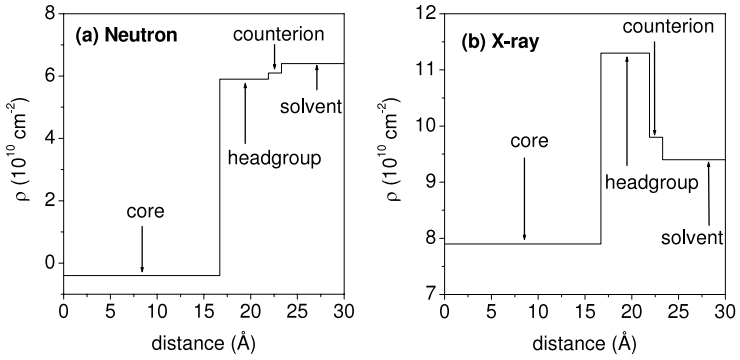

Figure 2. The variation in the scattering length density for different components of LiDS micelles: (a) neutron and (b) x-ray scattering. The profiles are given along the minor axis of the micelle.

to fit the SAXS data, and the thickness (t) of the condensed counterions around the micelle is obtained as an additional parameter. The parameters in the analysis were optimized by means of a nonlinear least-square fitting program [32].

4. Results and discussion

Figure 1 shows SANS and SAXS data from 0.3 M LiDS micellar solution. The Q dependence of the scattered intensity is very different for these two techniques. This can be understood in terms of different scattering contrasts for different components of the micelles as seen by the neutrons and x-rays (figure 2). The contrast for any component depends on the square of the difference of scattering length densities of that component and the solvent. It is clear from the variation in scattering length density for neutrons (figure 2(a)) that there exists a very strong contrast for the core of micelles in D_2O with respect to that from the head groups and counterions. This makes the scattering from the head groups and counterions negligible and neutrons only see the core of the micelles. On the other hand, for x-rays (figure 2(b)) there is

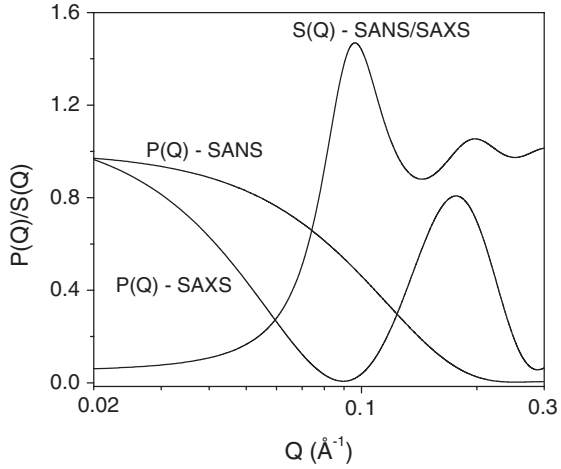

Figure 3. Fitted curves for $P(Q)$ and $S(Q)$ for SANS and SAXS data of LiDS micelles.

Table 1. Micellar parameters as obtained from SANS and SAXS for 0.3 M MDS.

Micellar system	Aggregation number (N)	Semi-minor axis $b = c$ (Å)	Semi-major axis a (Å)	Fractional charge (α)	Counterion condensation $1 - \alpha$ (%)	Head group thickness t_{hg} (Å)	Counterions thickness t (Å)
LiDS	79	16.7	23.6	0.31	69	5.3	—
NaDS	91	16.7	27.3	0.28	72	5.3	7.3
RbDS	144	16.7	43.3	0.13	87	5.3	5.3
CsDS	244	16.7	73.5	0.04	96	5.3	4.1

good contrast for the core of the micelles as well as the headgroups. The lithium counterion has a poor contrast. SANS data show a correlation peak at 0.09 A^{-1} which is due to a peak in the inter-particle structure factor $S(Q)$. The peak usually occurs at $Q_m \sim 2\pi/d$, where d is the average distance between the micelles [33]. The prominent peak of the SAXS data is observed at larger Q values and is due to the shell-like structure of the sulphate head groups around the micellar core [34]. The parameters of the analysis of SANS and SAXS data on LiDS micelles are given in table 1. SANS gives information about the structure (shape and size) and counterion condensation of the micelles. This information, as derived from SANS, is used to analyse the SAXS data, and the thickness of the headgroup shell (t_{hg}) is obtained. The fitted curves of $\langle F^2(Q)\rangle$ and $S(Q)$ for SANS and SAXS data of the 0.3 M LiDS micellar system are shown in figure 3.

SANS and SAXS data from the 0.3 M CsDS micellar solution are shown in figure 4. The general features of the data for 0.3 M CsDS are similar to those for 0.3 M LiDS micelles. The correlation peak in the SANS data of CsDS occurs at a significantly smaller Q value than that for LiDS, which is an indication of the formation of larger micelles with Cs^+ counterions. The large contribution of the scattering intensity in the lower Q region for SAXS data of 0.3 M CsDS is due to the large size of the micelles formed in this system. Figure 5 shows the contrast for different components of the micelles of CsDS, as seen by the neutrons and x-rays. It is clear that, unlike LiDS, the counterions of CsDS have a very strong contrast for x-rays. The values of the fitted parameters of the shape, size from SANS data and the thickness of the $-SO_4^-$ headgroup shell from LiDS data have been used to determine the thickness of Cs^+

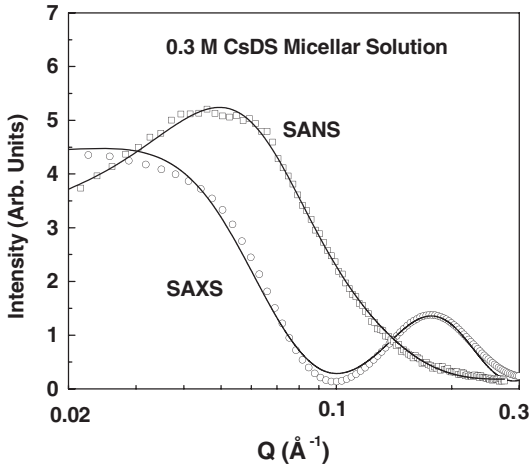

Figure 4. SANS and SAXS data from 0.3 M CsDS micellar solution. Points represent the experimental data and the solid lines are the theoretical fits to the data.

condensed counterions (t_{cc}) around the charged headgroups. The distribution of condensed counterions is treated as a step function and it fits the data reasonably well, perhaps due to the large condensation of the counterions on the charged micelles. The fitted parameters are given in table 1. The calculated curves of $\langle F^2(Q)\rangle$ and $S(Q)$ for SANS and SAXS data of the 0.3 M CsDS micellar system are shown in figure 6.

SANS data for 0.3 M alkali metal dodecyl sulphate (MDS) micellar solutions having different counterions (M^+) for NaDS, RbDS and CsDS are shown in figure 7. It is observed that the correlation peak broadens and shifts to lower Q values, along with an increase in the scattering intensity as the counterion is varied from Na^+ to Cs^+. These observations suggest that the micellar size and the interaction between the micelles depend strongly on the nature of the counterions [11–14]. Figure 8 shows the SAXS data on the same samples, for which the SANS data are shown in figure 7. Both peaks in the SAXS data show a significant change in the variation of the counterions. The change in correlation peak in the SAXS data follows a trend that is similar to that in the SANS data. However, the increase in the magnitude of the second peak corresponds to the enhancement of the contrast of condensed counterions due to an increase in the Z value of the counterions. The micellar parameters of the combined SANS and SAXS studies in these systems are given in table 1. It is seen that the fractional charge α on the micelle decreases and the aggregation number increases on the variation of counterions from Na^+ to Cs^+. The thickness of the condensed counterion shell decreases as the counterions are varied from Na^+ to Cs^+.

The hydrated size of the counterion plays an important role in deciding the structure and interaction in the micellar solutions. It is believed that, while counterions having higher hydration have more affinity to remain in the bulk of the micellar solution, the counterions having less hydration tend to stay near the micelle, and thereby, as the hydration of counterions decreases, their condensation increases and they provide a better screening of the micellar charge. The amount of charge neutralization at the surface of the micelle decides the effective head-group area and this controls the size and aggregation of the micelles. Our results using combined SANS and SAXS studies in these systems show that counterion condensation increases and the thickness over which they are condensed decreases with a decrease in the hydrated size of the counterions. This leads to the strong charge neutralization on the

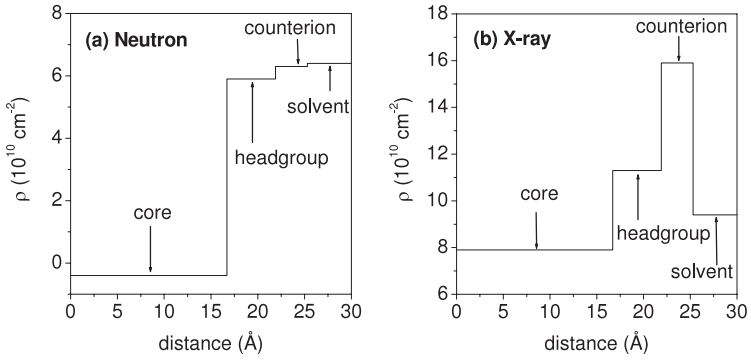

Figure 5. The variation of the scattering length density for different components of CsDS micelles (a) neutron and (b) x-ray scattering. The profiles are given along the minor axis of the micelle.

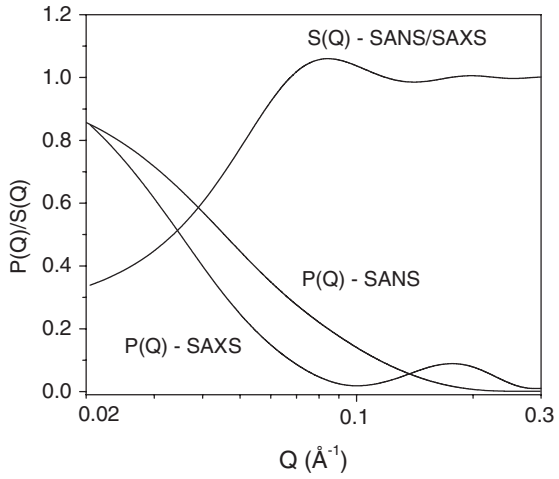

Figure 6. Fitted curves for $P(Q)$ and $S(Q)$ for SANS and SAXS data of CsDS micelles.

micellar surface and hence the formation of a larger size of micelles for smaller hydrated size counterions. Due to the fact that larger ions are less hydrated [7], the Cs^+ counterions are more effective in charge neutralization compared to Rb^+ and Na^+ counterions.

5. Conclusions

The effect of a variation of counterions on charged micelles of anionic surfactants of alkali metal dodecyl sulphate (MDS) for the counterions M = Li, Na, Rb and Cs has been examined by combined SANS and SAXS studies. While neutrons see the core of the micelle, x-rays give information on the counterion condensation around the micelle. It is found that the differences in the condensation of counterions around the micelles give rise to a different structure of the micelles. The size of the micelles increases with an decrease in the hydrated size of the counterion because of the increase in the counterion condensation and a decrease in the thickness over which they are condensed for smaller counterions.

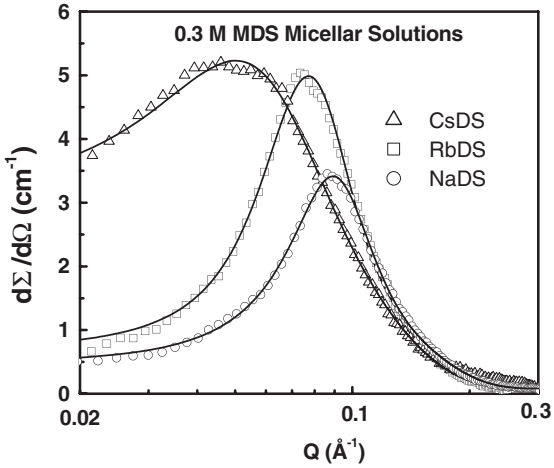

Figure 7. SANS Data from 0.3 M MDS with different counterions M = Na, Rb and Cs. Experimental data are represented by the points and the solid lines are the theoretical fits to the data.

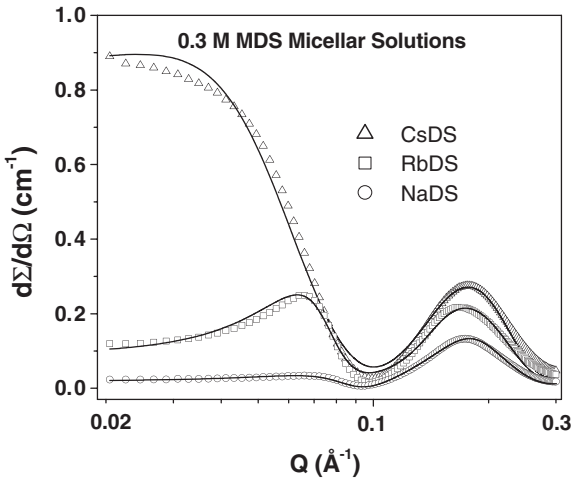

Figure 8. SAXS data from 0.3 M MDS with different counterions M = Na, Rb and Cs. Experimental data are represented by the points and the solid lines are the theoretical fits to the data.

Acknowledgments

The authors wish to thank Drs S Finet and T Narayanan for their kind help during the SAXS experiments at ESRF.

References

[1] Tanford C 1980 *The Hydrophobic Effect: Formation of Micelles and Biological Membranes* (New York: Wiley)
[2] Lindman B and Wennerstrom H 1980 *Top. Curr. Chem.* **87** 1

[3] Degiorgio V and Corti M 1985 *Physics of Amphiphiles: Micelles, Vesicles and Microemulsion* (Amsterdam: North-Holland)
[4] Zana R 1987 *Surfactant Solutions: New Methods of Investigation* (New York: Dekker)
[5] Chevalier Y and Zemb T 1990 *Rep. Prog. Phys.* **53** 279
[6] Chen S H 1986 *Annu. Rev. Phys. Chem.* **37** 351
[7] Israelachvili J N 1992 *Intermolecular and Surface Forces* (New York: Academic)
[8] Ramanathan G V 1988 *J. Chem. Phys.* **88** 3887
[9] Belloni L 1998 *Colloids Surf.* A **140** 227
[10] Aswal V K, Goyal P S, Amenitsch H and Bernstorff S 2004 *Pramana J. Phys.* **63** 333
[11] Sheu E Y, Wu C F and Chen S H 1986 *J. Phys. Chem.* **90** 4179
[12] Berr S S and Jones R R M 1988 *Langmuir* **4** 1247
[13] Aswal V K and Goyal P S 2000 *Phys. Rev.* E **61** 2947
[14] Joshi J V, Aswal V K, Bahadur P and Goyal P S 2002 *Curr. Sci.* **83** 47
[15] Mortensen K 1998 *Curr. Opin. Coll. Interface Sci.* **3** 12
[16] Pedersen J S and Svaneborg C 2002 *Curr. Opin. Coll. Interface Sci.* **7** 158
[17] Aswal V K and Goyal P S 2004 *Pramana J. Phys.* **63** 65
[18] Hamely I W and Castelletto V 2004 *Prog. Polym. Sci.* **29** 909
[19] Wu C F, Chen S H, Shih L B and Lin J S 1988 *Phys. Rev. Lett.* **61** 645
[20] Aswal V K, Goyal P S, De S, Bhattacharya S, Amenitsch H and Bernstoff S 2000 *Chem. Phys. Lett.* **329** 336
[21] Vass S, Plestil J, Laggner P, Gilanyi T, Borbely S, Kriechbaum M, Jakli G, Decsy Z and Abuja P M 2003 *J. Phys. Chem.* B **104** 12752
[22] Aswal V K, Kohlbrecher J, Goyal P S, Amenitsch H and Bernstorff S 2006 *J. Phys.: Condens. Matter* **18** 11399
[23] Berr S S 1987 *J. Phys. Chem.* **91** 4760
[24] Aswal V K and Goyal P S 2000 *Curr. Sci.* **79** 947
[25] Narayanan T, Diat O and Bösecke P 2001 *Nucl. Instrum. Methods Phys. Res.* A **467** 1005
[26] Lindner P and Zemb T 1991 *Neutron, X-Ray and Light Scattering: Introduction to an Investigative Tool for Colloidal and Polymeric Systems* (Amsterdam: North-Holland)
[27] Hayter J B and Penfold J 1983 *Colloid Polym. Sci.* **261** 1022
[28] Chen S H and Lin T L 1987 *Methods of Experimental Physics* vol 23B ed D L Price and K Skold (New York: Academic) p 489
[29] Pederson J S 1997 *Adv. Colloid Interface Sci.* **70** 171
[30] Egelstaff P A 1967 *An Introduction to Liquid State Physics* (London: Academic)
[31] Hayter J B and Penfold J 1981 *Mol. Phys.* **42** 109
[32] Bevington P R 1969 *Data Reduction and Error Analysis for Physical Sciences* (New York: McGraw-Hill)
[33] Chen S H, Sheu E Y, Kalus J and Hoffmann H 1988 *J. Appl. Crystallogr.* **21** 751
[34] Cabane B, Duplessix R and Zemb T 1985 *J. Physique* **46** 2161